Molecular Correlations between Breast Cancer and Diabetes Mellitus Type 2 Examined by *In Silico* analyses and Drug Inhibitory Effects

Farzaneh Afzali[1], Zahra Nayeri[1], Zarrin Minuchehr[2], Mossa Gardaneh[1*]

[1]Department of Medical Biotechnology, [2]Department of Systems Biotechnology, National Institute of Genetic Engineering and Biotechnology (NIGEB), Tehran, Iran.

***Corresponding author: Mossa Gardaneh**

National Institute of Genetic Engineering and Biotechnology, Pazhoohesh Blvd, Tehran-Karaj HWY Kilometer 15, PO BOX 14965/161, Tehran-Iran,

Tel: (+98) 21 44787 344

Fax: (+98 21) 4458-0395

Email: mossa65@nigeb.ac.ir, mossabenis65@gmail.com

ABSTRACT

Background: Nearly 16% of people with breast cancer (BC) have Diabetes Mellitus type 2 (DM2) and are at a higher risk of death worldwide. However, their common regulatory factors and functional mechanisms have not been profoundly understood. In this study, we used *in silico* approaches to study their co-regulated differentially expressed genes (DEGs) in order to explore and introduce novel therapeutic targets.

Results: Microarray analysis identified 196 co-regulated DEGs (156 upregulated and 40 downregulated) between BC and DM2. The most significant pathway was predicted to be *Fc gamma R*-mediated phagocytosis through pathway analysis. Through protein-protein interaction network investigation based on the co-regulated DEGs and performing topological characterization, common hubs were revealed. Then hubs' regulatory factors including TFs and miRNAs were also mined to introduce unprecedented therapeutic targets. According to Gene Ontology analysis, cell death and migration related processes found to be important enough for designing *in vitro* experiments. Co-treatment of Metformin (MTFN) and Curcumin (CURC) was the main inhibitory strategy we adopted as they both have impact on BC and DM2. Drug treatment was performed on two BC cell lines (MCF7 and MDA-MB-231). Combination index calculation by MTT viability assay proved additive effects and slight synergism on both cell lines. The superior apoptotic potential of co-treatment compared to single treatments was shown on inhibition of MCF7 proliferation and induction of cell death demonstrated by cell body co-staining and flow cytometry as well as gene expression analysis via RT-PCR. Furthermore, wound-healing scratch assay showed that this co-treatment has a slightly higher effect on migration inhibition compared to single treatments.

Conclusion: In conclusion, our study used *in silico* approaches and introduced a regulatory panel between BC and DM2. We also proved that our co-treatment inhibitory strategy successfully controlled the biological processes under investigation.

Keywords: metformin, curcumin, diabetes, breast cancer, in silico

Background

Hard-to-cure human diseases such as diabetes, cancer or neurodegenerative disorders are often multifactorial in nature implying that a diverse range of underlying mechanisms behind disease genesis and progression need to be taken into consideration for improved management. Multi-factorial mechanisms of disease development involve multi-gene complexes that are best functional within their appropriate biological networks including any related pathways, processes, functions or even their niche of existence (1). An important manifestation of these biological networks is shown by gene regulatory networks that provide functional explanations for many biological phenomena and pathological conditions by identifying key molecules, their relevant pathways, and their causative relationships (2). Once disease causes are identified, solutions for disease management and therapy become readily traceable. Therefore in the context of multi-factorial diseases, multi-target ideas based on targeting either multiple factors or conditions are amplified. Such multi-target strategies are indeed more beneficial to patients than single-target procedures for heterogeneous diseases of diabetes mellitus type 2 (DM2) or breast cancer (BC) that are also influenced by global factors like environment or lifestyle (3).

BC and DM2 fuel one another's occurrence considering their common underlying pathways of glucose metabolism. The impaired metabolism of abundant glucose and its related cascades constitutes the basis of the "Warburg effect" theory (4, 5). The Warburg effect states that, despite

bioavailability of oxygen for effective ATP production via oxidative phosphorylation, cancer cells initiate less-productive glycolysis to produce their required energy fuel. Glycolysis does not produce enough ATP but the cell experiences up-regulation of genes responsible for absorbing more glucose known as metabolic reprogramming (6, 7). Metabolic reprogramming plays critical roles particularly in adaptation of cancer cells to restrictive conditions dictated by tumor microenvironment. The Warburg effect is triggered by up-regulation of molecules such as GLUT proteins that promote glucose transfer across cell membrane and accumulation of cytosolic glucose (8).

Metformin (N',N'-dimethyl biguanide hydrochloride; MTFN) and curcumin (1,7-bis(4-hydroxy-3-methoxyphenyl)-1,6-heptadiene-3,5-dione; CURC) both have inhibitory effects on DM2 and BC, a criterion needed for our study. As an anti-DM2 drug, MTFN suppresses hyperinsulinemia and hyperglycemia by counteracting insulin resistance in DM2. MTFN inhibits gluconeogenesis and so glucose absorption from the small intestine and increases glucose uptake in the cells and reduces plasma free fatty acid concentration (9). MTFN also increases insulin induced translocation of glucose transporters to the cell membrane and so reduces insulin resistance (8). The anti-mitogenic effects of MTFN on cancer cells are exerted either by activating intracellular energy sensor adenosine monophosphate-activated protein kinase (AMPK) or via AMPK-independent signaling pathways (10). Major impacts of MTFN on cancer include sensitization of resistant tumors to chemo-radio- and antibody- therapy (11-13) which are mainly caused by selective killing of tumor-initiating cells or cancer stem cells (CSCs) by MTFN (14). Such resensitizing potential of MTFN has been shown to improve the prognosis of diabetic patients who carry HER2+ BC tumors (15). Combined with cancer drugs such as cisplatin or doxorubicin, MTFN indeed enhances their cytotoxicity and such combination synergistically

reduces tumor size (16), an unexplored potential of MTFN that is being examined in clinical trials (17).

Curcumin (CURC) induces cancer cell death by a long list of inhibitory and inducing activities on cellular pathways involved in apoptosis, autophagy and growth inhibition (18). Reduced cell growth, arrested cell cycle and diminished tumor size and inhibited metastasis are effects of CURC on HER2+ BC xenografts (19). Our own study indicates that CURC can synergize with TZMB as well as with anti-oxidant enzyme glutathione peroxidase-1 in inducing apoptosis in HER2-overexpressing BC cells, indicating CURC potential to challenge TZMB (20). Furthermore, Kakarala et al have demonstrated that CURC can be used to target CSCs in BC (21). On the other hand, CURC affects glucose metabolism by inhibiting aerobic glycolysis in cancer cells (22).

Together, MTFN and CURC appear to have converging points to synergize in halting tumorigenicity as a whole but also each can affect specific molecules or pathways within cancer cells. Co-treatment with MTFN and CURC indeed inhibits cancer growth, metastasis, and angiogenesis *in vitro* and *in vivo* (23), and inhibits angiogenesis, modulates immune system and induces apoptosis independent from p53 in BC (24).

The aim of our current study is to explore fortifying effects of MTFN and CURC on inhibiting the redundant processes achievable by *in silico* studies. We initially identified targetable elements for both BC and DM2 by analyzing their inter-network correlations based on which inhibiting treatments can be adapted to control redundant joint processes. Our next step was to adjust MTFN/CURC co-effects on Phosphatase and tensin homolog (PTEN) which is down-regulated upon MTFN treatment. PTEN is a tumor suppressor gene that antagonizes the PI3K/Akt/mTOR (25, 26). If occurs, up-regulation of PTEN expression could be another anti-

cancer dimension of MTFN/CURC co-treatment and diminishing their high-dose usage in single treatments.

METHODS

Microarray Analysis and Network Construction

Two high quality microarray datasets of human BC and DM2 were selected from the NCBI Gene Expression Omnibus (GEO): GSE65194 for BC (has various subtypes of BC: triple negative (TN), luminal A, luminal B and Her_2^+) and GSE95849 for DM2 (for datasets information refer to Additional file 1) (27-30). The differentially expressed genes (DEGs) were identified by applying RMA algorithm in R Studio v1.1.442. The genes with adj.p.val less than 0.05 and logFC > 1 or logFC < 1 were considered as DEGs. The co-regulated DEGs were obtained through logFC screening upon joint DEGs between BC and DM2.

The co-regulated DEGs were subjected to STRING database (31) to form the protein-protein (PPI) network. The cut-off of 0.7 applied and text mining was excluded as the reliable source to get the proper amount of interactions between proteins. The resulted network was imported in Cytoscape 3.6.0 and the NetworkAnalyzer tool was used to characterize its topological features. The Degree parameter was used as the connectivity index which considers the genes' neighbors to identify the hubs.

Mining Regulatory Factors and Performing Enrichment Analysis

The hubs were subjected to CyTargetLinker plugin (32) of Cytoscape 3.6.0 and TF2DNA server (33) (Kulakovskiy 2013, Jolma 2013, Weirauch 2014, and Mathelier 2014 were selected as curated sources) to introduce the related miRNAs and TFs respectively. The introduced miRNAs

were filtered by curated miRNAs of diabetes and BC available in miR2Disease database (34). The TFs were also filtered by obtained DEGs of BC and DM2 in the current study.

To understand the biological meaning behind the co-regulated DEGs, we performed KEGG pathway and Gene Ontology (GO) analysis using DAVID 6.7 server (35). The output was divided into three charts named Molecular Function (MF), Biological Processes (BP) and Cellular Compartment (CC). The GO Terms were then filtered by *p* value less than 0.05 and the most significant GO terms were selected to be introduced. In parallel, by examining the BP list, we subjected important processes to our subsequent experiments *in vitro*.

Cell Culture

Human BC cell lines MCF7 (Michigan Cancer Foundation-7) and MDA-MB-231 (Michigan Cancer Foundation-7) were cultured in Dulbecco's modified eagle's medium (DMEM) plus 10% fetal calf serum (FBS), 100 U/mL penicillin, and 100 µg/mL streptomycin and incubated at 37 □C, 5 % CO2. MTFN and CURC were both purchased from Sigma-Aldrich and dissolved in DMSO to form treatment stocks.

MTT Viability Assay

The assay was carried out as we have reported (36). Serial concentrations of MTFN ranging from 5 to 21 mM and of CURC in the range of 5-21 µM were applied and DMSO as their solvent and positive control was used in parallel. The treated cells were incubated for 24 hours before incubating with the MTT solution in shaker for 30 min and reading by an ELISA reader at 580 nm wavelength. The calculated IC50 represents the treatment concentration that inhibits the growth of 50% of cells versus control cells.

Measurement of Synergism and Antagonism

We used Minitab 16 Statistical Software as a tool to design the contribution of each drug in combination. The Response Surface was used as the experiment design type. As we had two drugs (two factors), the central composites made 13 ways of co-treatment. To determine lower and higher dose of each drug, we chose axial point level to exactly draw the experiments between these concentrations. To gain more specific doses, doses of single treatments were applied and the range was narrowed to 9-13 mM for MTFN and 5-6 μM for CURC. We then calculated combination index (CI) for the two compounds using formula below and as we have described (20):

$CI = (D_1/Dx_1) + (D_2/Dx_2) + (D_1D_2/Dx_lDx_2)$, where Dx_1 and Dx_2 represent the doses of MTFN and CURC alone needed to produce x percentage effect, and D_1 and D_2 indicate the doses of MTFN and CURC in combination required to produce this effect.

Acridine Orange/Ethidium Bromide (AO/EB) Co-staining

Cells were co-stained according to our previous reports (37). We applied the IC_{50} of MTFN, CURC and of their combination as inhibitory treatments. The images of stained cells were captured using fluorescent microscope.

Flow Cytometry Evaluation of Cell Death by Annexin V-FITC/PI Double Labeling

MCF7 cells were seeded 2×10^5 per well in a 6 well plate. After treatments, the cells were trypsinized, were resuspended and were incubated with the stains for 5 min at room temperature before being analyzed by a FACSCalibur at 488 nm wavelength. A total of 10,000 cells were used per sample and the data were analyzed in FlowJo 7.6.1.

Reverse Transcription (RT) PCR

RT-PCR analysis was carried out as previously described (36). The primer pairs used for GAPDH as control, BAX, BCL2, and PTEN are as follows: *GAPDH:* 5'-CCCCCAATGTATCCGTTGTG-3' and 5'-TAGCCCAGGATGCCCTTTAGT-3' (Accession: NG_007073); *BAX:* 5'-TGG AGCTGCAGAGGATGATTG-3' and 5'-GAAGTTGCCGTCAGAAAACATG-3' (Accession: NG_012191); *BCL2*: 5'-CTGCACCTGACGCCCTTCACC-3' and 5'-CACATGACCCCACCGAACTCAAAGA-3' (Accession: NG_009361), and *PTEN*: 5'- CGAACTGGTGTAATGATATGT-3' and 5'-CATGAACTTGTCTTCCCGT -3' (Accession: NG_007466). The reaction products were then visualized using Gel Electrophoresis and quantified using ImageJ1.51 software (38).

Wound Healing/ Scratch Assay

One day after seeding 3×10^5 MCF7 cells on each well of a 6-well plate, a scratch was made by a micropipette yellow tip and the cells were washed and re-fed with serum-free medium. The Cells' images were taken before and after treatment period and were analyzed using ImageJ software. The area between two sides of each wound was measured for monitoring cell migration.

Statistical Analysis

The experimental data were analyzed by GraphPad Prism 6 and was provided as mean ± standard deviation (SD) of two independent experiments. The significance of differences between groups was analyzed by paired *t-test*. We considered p value less than 0.05 as significant, and p value less than 0.01 or 0.001 as highly significant.

Results

1. Network of co-regulated genes between BC and DM2

The DEGs of BC (all subtypes luminal A, luminal B, TN, Her2^{+}) and DM2 were 2886 and 2299 respectively. After merging the data, a list of 196 co-regulated genes (156 upregulated and 40 downregulated) was obtained (Additional file 1).

The imported PPI network possessed 63 nodes and 60 edges. The resulted Degrees following topological characterization of PPI network were monitored and the top 12 nodes (20 percent of the whole nodes) were introduced as hubs (Table 1).

2. The regulatory panel of co-regulated DEGs

The experimentally approved, mined and filtered TFs and miRNAs of identified hubs were visualized by Cytoscape 3.6.0 (Fig. 1). The related biological processes (BP) were also revealed by GO analysis. The regulatory panel is available in Table 1 along the hubs' expressional status.

3. Biological processes used in our in vitro experiments

GO enrichment analysis held on co-regulated DEGs to introduce cellular concentration, function, and also redundant processes that can be targets of in-vitro experiments. Considering *p* value less than 0.05, the most important GO terms of molecular function and cellular component were IgG binding (GO:0019864) and Golgi apparatus (GO:0005794), respectively. The critical biological process was protein localization (GO:0008104). By analyzing the BP list, it was found that cell death and migration related processes were repeated so frequently that worth being analyzed under inhibiting treatments. The *Fc gamma* R-mediated phagocytosis was predicted to be the most enriched pathway between BC and DM2 (Table 2; for the complete list refer to Additional file 2).

4. Severe anti-proliferative effect of MTFN-CURC co-treatment on BC cell lines

MTT viability assay showed a significant difference (less than 0.001) between drug-treated cells and their DMSO-treated controls. We considered this difference a net effect of drugs. The IC_{50} of MTFN was 19 mM for MCF7 and 21 mM for MDA-MB-231. As for CURC, these figures stood at 13 μM and 15 μM, respectively (Fig. 2A). To better annotate if the drugs would support each other, we calculated their CI50. It was found that co-treatment more powerfully inhibits BC cell proliferation than single treatments. As both cell lines were responsive to single treatments, we measured the CI_{50} of either drug in co-treatment studies. The CI_{50} of MTFN was 11 mM in MCF7 and 12 mM in MDA-MB-231 whereas that of CURC stood at 5 μM in both lines (Fig. 2B). The IC_{50} and CI values and definitions are shown in Table 3. To ensure the anti-proliferative or apoptotic nature of the observed reduced cell survival, AO/EB co-staining was performed.

5. Increased Growth Inhibition and Apoptotic Cell Death in Co-treated MCF7

Metformin-treated MCF7 cells exhibited proliferation inhibition and morphology changes from spindle shape to circular. Acridine orange/ethidium bromide (AO/EB) co-staining showed some yellow/green and partially orange cells as sign of apoptosis (Fig. 2C). CURC-treated dead cells outnumbered MTFN-treated ones. We also detected plenty of fully orange cells as sign of Necrosis. The number of cells remaining in co-treated wells was minimum indicating more profound effect of co-treatment on killing cells compared to single treatments.

Annexin V-FITC/PI double labeling fluorescence followed by flow cytometry was applied to more precisely monitor apoptosis among treated cells. As shown in Fig. 3A, CURC is more potent in killing cells so that it eradicated 35.74% of the treated BC cells compared to 24.81% killed by MTFN alone. Conversely, MTFN left 75.2% of cells alive whereas percent of live cells upon CURC treatment was 64.3%. The data demonstrate that proliferation inhibition is the

dominant strategy MTFN adopts to stop cancer cell growth. We comprehended that co-treatment is more efficient against cancerous cells by inducing apoptosis (40.68%) more than single treatments.

Another way to ensure this finding is analyzing whether co-treatment alters apoptotic genes expression more than single treatments or not. As you see in Fig. 3B, both on electrophoresis gel and quantified chart, co-treatment significantly reduces expression of BCL2 as an anti-apoptotic gene and has slightly more effect on increasing expression of BAX as a pro-apoptotic gene. It also improves PTEN expression versus MTFN treated cells that is another proof for better effect of co-treatment in inducing anti-cancer effects because PTEN is a tumor suppressor.

6. Superior Effect of Co-treatment on Migration

Figure 4, demonstrates the pattern of BC cell migration in 24 h of being under the impact of applied drugs regarding the wound area. The result of these experiments showed that both single and co-treatments constrain cells' movement, but co-treatment is a little more efficient rather than single treatments.

Discussion

In the current study, we mapped the common regulatory factors behind two deadly human disorders BC and DM2 by analyzing microarray datasets, mining TFs, annotating miRNAs, and performing GO analysis. We introduced a regulatory panel containing 12 hubs and their related TFs and miRNAs as the most crucial factors responsible for the occurrence of these conditions. The MTFN/CURC co-treatment exerted anti-proliferative effects, including both cell death and growth inhibition, on cancer cells that were manifested as slightly synergistic on MDA-MB-231 and additive on and MCF7 cell lines. The expression of BCL2 was decreased while that of BAX was increased under MTFN/CURC co-treatment compared to single treatments. Also, PTEN was

overexpressed by co-treatment versus MTFN single treatment. Finally, the co-treatment promoted migration inhibition slightly more than single treatments did.

BC heterogeneity that drives tumorigenesis, metastasis, recurrence, and drug resistance necessitates drugs combinatory and multi-target strategies to be adopted for BC tumor cure. The gene expression profiling, regulatory genes, and pathways involved in this phenomenon need to be taken to account for ultimate solutions (39). Metabolic disorders like DM2 that result from desk-bound activities, also, are responsible for BC emergence and evolvement (40, 41). In DM2, insulin resistance or scarcity of insulin production enhances glucose level in blood (42) and as a sign of BC-DM2 adjoining, the extra glucose will be consumed by cancerous cells as their fuel to survive and grow.

Our pathways analysis revealed FcγR-mediated phagocytosis as one of those pathways significantly shared between BC and DM2. The FcγR family is responsible for phagocytosis, activating macrophages, exuding reactive oxygen intermediates (ROIs), and having cytotoxic effect on tumors attached to antibodies (43). On one hand, FcγRI is directly involved in cancer immune antibody therapies that reduce tumor size including antibody-dependent cellular phagocytosis and antibody-dependent cellular cytotoxicity (44, 45). On the other hand, the monocytes of DM2 patients fail to properly promote FcγR-mediated phagocytosis, a problem that results in elevated blood glucose levels. This dysfunction shows direct correlations between DM2 and defected immune system (46). In line with the hubs' BP list that proposes distinct immune system processes, we propose that by targeting the identified immune biomarkers and pathways, the inflammatory cascades would be captured and the occurrence of both diseases would be decreased.

Mitochondrial dysfunction involved in intrinsic apoptotic pathways relevant to tumor formation contributes to development of both BC and DM2 (47-49). We and others have reported reduced BCL2 expression and increased BAX expression by CURC and MTFN single treatments (50, 51). Now, our current study reports that CURC-MTFN co-treatment more significantly induces BCL2 downregulation and BAX upregulation, hence inducing apoptosis more efficiently compared to single treatment. We found that MTFN adopts a strategy of inhibiting proliferation rather than inducing cell death. This may be due to MTFN ability to reduce circulating insulin leading to downregulation of proliferation pathways that are physiologically triggered by insulin or insulin growth factors (52). The findings were quantified by AnnexinV-FITC/PI double labeling in flow cytometry that confirmed MTFN proliferation inhibition and co-treatment cell death induction.

PTEN plays complex roles in multiple cellular processes including proliferation, survival, apoptosis, cell cycle regulation, adhesion, and migration (25, 53). In our study, PTEN expression was reduced upon MTFN treatment but this reduction was compensated following MTFN/CURC co-treatment. Cell death induction by co-treatment suggests that the co-presence of MTFN and CURC may support the tumor-suppressing function of PTEN. Beside its anti-tumor activity, PTEN can also restrain Akt/PI3K pathway and so act as a negative regulator of proliferation (54). This restriction may downregulate or abate the insulin signaling pathway and result in insulin accumulation, insulin resistance, and hyperglycemia thereby co-promoting DM2 and BC. Therefore, PTEN reduction can help in the optimal use of insulin in cells (55, 56). MTFN promotes PTEN down-regulation through AMPK dependent mode (52) and beside its anti-DM2 effects, controls BC indirectly via the Warburg effect. The AMPK pathway acts as a sensor of energy in cells and further plays a major role in insulin signaling (57-59).

Cell metastasis is a major complexity that makes cancer hard to control. Both MTFN and CURC have anti-metastatic effect on cancer cells (60, 61). The wound healing assay we carried out showed more efficient but insignificant differences in cell migration in our MTFN/CURC co-treated samples compared to single treatments. MTFN and CURC effects on angiogenesis genes that help the migration phenomenon are controversial and cell-dependent especially in BC (62-66). Therefore, further investigations are needed to monitor changes in the expression of specific genes in migration-related pathways so to understand the mechanisms associated with this co-treatment.

Conclusion

In conclusion, we produced bioinformatics data that were compatible with our experimental ones on MTFN/CURC co-treated BC cell lines. Our diverse experiments showed that the proposed co-treatment inhibitory strategy is more effective than single treatments. The xenografts' tumors derived from BC patients who also suffer DM2 provide suitable *in vivo* models for simultaneous evaluation of this co-treatment on both conditions. Also, the expression evaluation of involved factors in the introduced regulatory panel can be another phase of study to fully comprehend the underlying mechanisms.

Declarations

- **Availability of data and material:** The microarray datasets analyzed during the current study are available in the GEO repository, [https://www.ncbi.nlm.nih.gov/geo/query/acc.cgi?acc=GSE65194, https://www.ncbi.nlm.nih.gov/geo/query/acc.cgi?acc=GSE95849]
- **Competing interests:** The authors declare that they have no competing interests
- **Funding:** This study was financially supported by a grant (502) from NIGEB.

- **Authors' contributions:** FA has done much of the experimental work as her MSc thesis. ZN has explored the tools for in-silico strategies and helped FA to design these experiments. ZM has designed the important parts of bioinformatics studies and supervised FA to carry out relevant investigations. MG was FA's supervisor, grantee and designer of the whole study.
- **Acknowledgements:** Not applicable

References

1. Stolk RP, Rosmalen JG, Postma DS, de Boer RA, Navis G, Slaets JP, et al. Universal risk factors for multifactorial diseases. European journal of epidemiology. 2008;23(1):67-74.
2. Kheitan S, Minuchehr Z, Soheili Z-S. Exploring the cross talk between ER stress and inflammation in age-related macular degeneration. PloS one. 2017;12(7):e0181667.
3. Giordano S, Petrelli A. From single-to multi-target drugs in cancer therapy: when aspecificity becomes an advantage. Current medicinal chemistry. 2008;15(5):422-32.
4. Larsson SC, Mantzoros CS, Wolk A. Diabetes mellitus and risk of breast cancer: a meta-analysis. International journal of cancer. 2007;121(4):856-62.
5. Lu H, Forbes RA, Verma A. Hypoxia-inducible factor 1 activation by aerobic glycolysis implicates the Warburg effect in carcinogenesis. Journal of Biological Chemistry. 2002;277(26):23111-5.
6. Hsu PP, Sabatini DM. Cancer cell metabolism: Warburg and beyond. Cell. 2008;134(5):703-7.
7. Warburg O. On the origin of cancer cells. Science. 1956;123(3191):309-14.
8. Singer K, Kastenberger M, Gottfried E, Hammerschmied CG, Büttner M, Aigner M, et al. Warburg phenotype in renal cell carcinoma: High expression of glucose-transporter 1 (GLUT-1) correlates with low CD8+ T-cell infiltration in the tumor. International journal of cancer. 2011;128(9):2085-95.
9. Chae YK, Arya A, Malecek M-K, Shin DS, Carneiro B, Chandra S, et al. Repurposing metformin for cancer treatment: current clinical studies. Oncotarget. 2016;7(26):40767.
10. Lei Y, Yi Y, Liu Y, Liu X, Keller ET, Qian C-N, et al. Metformin targets multiple signaling pathways in cancer. Chinese journal of cancer. 2017;36(1):17.
11. Vazquez-Martin A, Oliveras-Ferraros C, Del Barco S, Martin-Castillo B, Menendez JA. The anti-diabetic drug metformin suppresses self-renewal and proliferation of trastuzumab-resistant tumor-initiating breast cancer stem cells. Breast cancer research and treatment. 2011;126(2):355-64.
12. Iliopoulos D, Hirsch HA, Struhl K. Metformin decreases the dose of chemotherapy for prolonging tumor remission in mouse xenografts involving multiple cancer cell types. Cancer research. 2011:canres. 3471.2010.
13. Song CW, Lee H, Dings RP, Williams B, Powers J, Dos Santos T, et al. Metformin kills and radiosensitizes cancer cells and preferentially kills cancer stem cells. Scientific reports. 2012;2:362.

14. Hirsch HA, Iliopoulos D, Tsichlis PN, Struhl K. Metformin selectively targets cancer stem cells, and acts together with chemotherapy to block tumor growth and prolong remission. Cancer research. 2009;69(19):7507-11.
15. Sonnenblick A, Agbor-Tarh D, Bradbury I, Di SC, Azim JH, Fumagalli D, et al. Impact of Diabetes, Insulin, and Metformin Use on the Outcome of Patients With Human Epidermal Growth Factor Receptor 2-Positive Primary Breast Cancer: Analysis From the ALTTO Phase III Randomized Trial. Journal of clinical oncology: official journal of the American Society of Clinical Oncology. 2017;35(13):1421-9.
16. Du J, Shi H-r, Ren F, Wang J-l, Wu Q-h, Li X, et al. Inhibition of the IGF signaling pathway reverses cisplatin resistance in ovarian cancer cells. BMC cancer. 2017;17(1):851.
17. Marrone KA, Zhou X, Forde PM, Purtell M, Brahmer JR, Hann CL, et al. A Randomized Phase II Study of Metformin plus Paclitaxel/Carboplatin/Bevacizumab in Patients with Chemotherapy-Naïve Advanced or Metastatic Nonsquamous Non-Small Cell Lung Cancer. The oncologist. 2018:theoncologist. 2017-0465.
18. Ravindran J, Prasad S, Aggarwal BB. Curcumin and cancer cells: how many ways can curry kill tumor cells selectively? The AAPS journal. 2009;11(3):495-510.
19. Lai H-W, Chien S-Y, Kuo S-J, Tseng L-M, Lin H-Y, Chi C-W, et al. The potential utility of curcumin in the treatment of HER-2-overexpressed breast cancer: an in vitro and in vivo comparison study with herceptin. Evidence-Based Complementary and Alternative Medicine. 2012;2012.
20. Gardaneh M, Shojaei S, Rahimi Shamabadi A, Akbari P. Breast Cancer Cell Apoptosis is Synergistically Induced by Curcumin, Trastuzumab, and Glutathione Peroxidase-1 but Robustly Inhibited by Glial Cell Line-Derived Neurotrophic Factor. Nutrition and cancer. 2018;70(2):288-96.
21. Kakarala M, Brenner DE, Korkaya H, Cheng C, Tazi K, Ginestier C, et al. Targeting breast stem cells with the cancer preventive compounds curcumin and piperine. Breast cancer research and treatment. 2010;122(3):777-85.
22. Wang K, Fan H, Chen Q, Ma G, Zhu M, Zhang X, et al. Curcumin inhibits aerobic glycolysis and induces mitochondrial-mediated apoptosis through hexokinase II in human colorectal cancer cells in vitro. Anti-cancer drugs. 2015;26(1):15-24.
23. Zhang HH, Zhang Y, Cheng YN, Gong FL, Cao ZQ, Yu LG, et al. Metformin incombination with curcumin inhibits the growth, metastasis, and angiogenesis of hepatocellular carcinoma in vitro and in vivo. Molecular carcinogenesis. 2018;57(1):44-56.
24. Falah RR, Talib WH, Shbailat SJ. Combination of metformin and curcumin targets breast cancer in mice by angiogenesis inhibition, immune system modulation and induction of p53 independent apoptosis. Therapeutic advances in medical oncology. 2017;9(4):235-52.
25. Chu EC, Tarnawski AS. PTEN regulatory functions in tumor suppression and cell biology. Medical Science Monitor. 2004;10(10):RA235-RA41.
26. Luo J, Manning BD, Cantley LC. Targeting the PI3K-Akt pathway in human cancer. Cancer cell. 2003;4(4):257-62.
27. Luo L, Zhou W-H, Cai J-J, Feng M, Zhou M, Hu S-P, et al. Gene expression profiling identifies downregulation of the neurotrophin-MAPK signaling pathway in female diabetic peripheral neuropathy patients. Journal of diabetes research. 2017;2017.
28. Maire V, Baldeyron C, Richardson M, Tesson B, Vincent-Salomon A, Gravier E, et al. TTK/hMPS1 is an attractive therapeutic target for triple-negative breast cancer. PloS one. 2013;8(5):e63712.
29. Maire V, Némati F, Richardson M, Vincent-Salomon A, Tesson B, Rigaill G, et al. Polo-like kinase 1: a potential therapeutic option in combination with conventional chemotherapy for the management of patients with triple-negative breast cancer. Cancer research. 2012:canres. 2633.012.
30. Maubant S, Tesson B, Maire V, Ye M, Rigaill G, Gentien D, et al. Transcriptome analysis of Wnt3a-treated triple-negative breast cancer cells. PloS one. 2015;10(4):e0122333.
31. STRING: functional protein association networks [Internet]. [cited 2017]. Available from: https://string-db.org/.

32. Kutmon M, Kelder T, Mandaviya P, Evelo CT, Coort SL. CyTargetLinker: a cytoscape app to integrate regulatory interactions in network analysis. PloS one. 2013;8(12):e82160.
33. TF2DNA database [Internet]. [cited 2017]. Available from: http://fiserlab.org/tf2dna_db//index.html.
34. miR2Disease Base [Internet]. [cited 2018]. Available from: http://watson.compbio.iupui.edu:8080/miR2Disease/index.jsp.
35. DAVID Bioinformatics Resources 6.7 [Internet]. [cited 2016]. Available from: https://david-d.ncifcrf.gov/.
36. Gardaneh M, Gholami M, Maghsoudi N. Synergy between glutathione peroxidase-1 and astrocytic growth factors suppresses free radical generation and protects dopaminergic neurons against 6-hydroxydopamine. Rejuvenation research. 2011;14(2):195-204.
37. Gharib E, Gardaneh M, Shojaei S. Upregulation of Glutathione Peroxidase-1 Expression and Activity by Glial Cell Line–Derived Neurotrophic Factor Promotes High-Level Protection of PC12 Cells Against 6-Hydroxydopamine and Hydrogen Peroxide Toxicities. Rejuvenation research. 2013;16(3):185-99.
38. Gassmann M, Grenacher B, Rohde B, Vogel J. Quantifying Western blots: pitfalls of densitometry. Electrophoresis. 2009;30(11):1845-55.
39. Yersal O, Barutca S. Biological subtypes of breast cancer: Prognostic and therapeutic implications. World journal of clinical oncology. 2014;5(3):412.
40. Peairs KS, Barone BB, Snyder CF, Yeh H-C, Stein KB, Derr RL, et al. Diabetes mellitus and breast cancer outcomes: a systematic review and meta-analysis. Journal of Clinical Oncology. 2011;29(1):40.
41. Wahdan-Alaswad R, Fan Z, Edgerton SM, Liu B, Deng X-S, Arnadottir SS, et al. Glucose promotes breast cancer aggression and reduces metformin efficacy. Cell cycle. 2013;12(24):3759-69.
42. Zheng Y, Ley SH, Hu FB. Global aetiology and epidemiology of type 2 diabetes mellitus and its complications. Nature Reviews Endocrinology. 2018;14(2):88.
43. Hutchinson M, Harrison PT, Floto RA, Allen JM. Fcγ receptor-mediated phagocytosis requires tyrosine kinase activity and is ligand independent. European journal of immunology. 1995;25(2):481-7.
44. Chokri M, Girard A, Borrelly M, Oleron C, Romet-Lemonne J, Bartholeyns J. Adoptive immunotherapy with bispecific antibodies: targeting through macrophages. Research in immunology. 1992;143(1):95-9.
45. Weiner LM, Moldofsky PJ, Gatenby RA, O'Dwyer J, O'Brien J, Litwin S, et al. Antibody delivery and effector cell activation in a phase II trial of recombinant γ-interferon and the murine monoclonal antibody CO17-1A in advanced colorectal carcinoma. Cancer research. 1988;48(9):2568-73.
46. Restrepo BI, Twahirwa M, Rahbar MH, Schlesinger LS. Phagocytosis via complement or Fc-gamma receptors is compromised in monocytes from type 2 diabetes patients with chronic hyperglycemia. PloS one. 2014;9(3):e92977.
47. Mohan S, Abdul AB, Abdelwahab SI, Al-Zubairi AS, Sukari MA, Abdullah R, et al. Typhonium flagelliforme induces apoptosis in CEMss cells via activation of caspase-9, PARP cleavage and cytochrome c release: Its activation coupled with G0/G1 phase cell cycle arrest. Journal of ethnopharmacology. 2010;131(3):592-600.
48. Rains JL, Jain SK. Oxidative stress, insulin signaling, and diabetes. Free Radical Biology and Medicine. 2011;50(5):567-75.
49. Riar AK, Kenny TC, Takabatake Y, Papa L, Germain D. Mitochondrial dysfunction in breast cancer. Research and Reports in Biology. 2015;6:137-45.
50. Chiu T-L, Su C-C. Curcumin inhibits proliferation and migration by increasing the Bax to Bcl-2 ratio and decreasing NF-κBp65 expression in breast cancer MDA-MB-231 cells. International journal of molecular medicine. 2009;23(4):469-75.

51. Yasmeen A, Beauchamp M-C, Piura E, Segal E, Pollak M, Gotlieb WH. Induction of apoptosis by metformin in epithelial ovarian cancer: involvement of the Bcl-2 family proteins. Gynecologic oncology. 2011;121(3):492-8.
52. Zakikhani M, Dowling R, Fantus IG, Sonenberg N, Pollak M. Metformin is an AMP kinase–dependent growth inhibitor for breast cancer cells. Cancer research. 2006;66(21):10269-73.
53. Di Cristofano A, Pandolfi PP. The multiple roles of PTEN in tumor suppression. Cell. 2000;100(4):387-90.
54. Lee SK, Lee JO, Kim JH, Kim SJ, You GY, Moon JW, et al. Metformin sensitizes insulin signaling through AMPK-mediated pten down-regulation in preadipocyte 3T3-L1 cells. Journal of cellular biochemistry. 2011;112(5):1259-67.
55. Stiles B, Wang Y, Stahl A, Bassilian S, Lee WP, Kim Y-J, et al. Liver-specific deletion of negative regulator Pten results in fatty liver and insulin hypersensitivity. Proceedings of the National Academy of Sciences. 2004;101(7):2082-7.
56. Wijesekara N, Konrad D, Eweida M, Jefferies C, Liadis N, Giacca A, et al. Muscle-specific Pten deletion protects against insulin resistance and diabetes. Molecular and cellular biology. 2005;25(3):1135-45.
57. Hardie DG, Carling D. The AMP-activated protein kinase: Fuel gauge of the mammalian cell? European journal of biochemistry. 1997;246(2):259-73.
58. Ju J-S, Gitcho MA, Casmaer CA, Patil PB, Han D-G, Spencer SA, et al. Potentiation of insulin-stimulated glucose transport by the AMP-activated protein kinase. American Journal of Physiology-Cell Physiology. 2007;292(1):C564-C72.
59. Zong H, Ren JM, Young LH, Pypaert M, Mu J, Birnbaum MJ, et al. AMP kinase is required for mitochondrial biogenesis in skeletal muscle in response to chronic energy deprivation. Proceedings of the national academy of sciences. 2002;99(25):15983-7.
60. Cerezo M, Tichet M, Abbe P, Ohanna M, Lehraiki A, Rouaud F, et al. Metformin blocks melanoma invasion and metastasis development in a AMPK/p53-dependent manner. Molecular cancer therapeutics. 2013:molcanther. 1226.2012.
61. Kunnumakkara AB, Anand P, Aggarwal BB. Curcumin inhibits proliferation, invasion, angiogenesis and metastasis of different cancers through interaction with multiple cell signaling proteins. Cancer letters. 2008;269(2):199-225.
62. Dallaglio K, Bruno A, Cantelmo AR, Esposito AI, Ruggiero L, Orecchioni S, et al. Paradoxic effects of metformin on endothelial cells and angiogenesis. Carcinogenesis. 2014;35(5):1055-66.
63. Farhangi B, Alizadeh AM, Khodayari H, Khodayari S, Dehghan MJ, Khori V, et al. Protective effects of dendrosomal curcumin on an animal metastatic breast tumor. European journal of pharmacology. 2015;758:188-96.
64. Phoenix KN, Vumbaca F, Claffey KP. Therapeutic metformin/AMPK activation promotes the angiogenic phenotype in the ERα negative MDA-MB-435 breast cancer model. Breast cancer research and treatment. 2009;113(1):101-11.
65. Shao ZM, Shen ZZ, Liu CH, Sartippour MR, Go VL, Heber D, et al. Curcumin exerts multiple suppressive effects on human breast carcinoma cells. International journal of cancer. 2002;98(2):234-40.
66. Wang J, Li G, Wang Y, Tang S, Sun X, Feng X, et al. Suppression of tumor angiogenesis by metformin treatment via a mechanism linked to targeting of HER2/HIF-1α/VEGF secretion axis. Oncotarget. 2015;6(42):44579.

Tables

Table 1. The regulatory panel of co-expressioned genes between BC and DM2.

Hub Symbol	Expression Status	Biological Processes	Regulator (miRNA)	Regulator (TF)
NCBP1	Up-regulated	• intracellular transport	hsa-let-7d hsa-let-7a hsa-miR-195 hsa-let-7i hsa-miR-377* hsa-let-7f hsa-miR-196a* hsa-miR-216a hsa-miR-98	DNMT1 PLAGL1 KLF6 ZNF219 KLF15
SEC24A	Up-regulated	• protein localization • establishment of protein localization • vesicle-mediated transport • cellular protein localization • cellular macromolecule localization • intracellular transport • membrane organization • Golgi vesicle transport	hsa-miR-182	ZFX HEY1 NFKB2 FOXO4 ETV5 USF2 TFAP2A YBX1
MAPK1	Up-regulated	• protein localization • intracellular signaling cascade • protein transport • small GTPase mediated signal transduction • protein kinase cascade • regulation of apoptosis • intracellular transport • regulation of cell death • MAPKKK cascade	hsa-miR-320 hsa-miR-22	TFCP2 STAT2 FOXP2 RAX2 TFE3 NR2F6 TFAP2A
RAC2	Up-regulated	• intracellular signaling cascade • small GTPase mediated signal transduction	hsa-miR-152 hsa-miR-181a* hsa-miR-181d	SPIB BCL6B MLXIPL

			hsa-miR-146a hsa-miR-148a	NFKB1 MESP1
OAS2	Up-regulated	• immune response	hsa-miR-181a* hsa-miR-18a	GABPA YY1 TFAP4
NCF2	Up-regulated	• immune response	hsa-miR-205 hsa-miR-136 hsa-miR-200c* hsa-miR-20a hsa-miR-7 hsa-miR-18a hsa-miR-200a* hsa-miR-200b*	IRF2 ESR1 IRF9 EHF NFKB1 STAT3 STAT1 TFAP4 RORA ERG
DMD	Down-regulated	• protein localization	hsa-miR-202* hsa-miR-29b hsa-miR-136 hsa-miR-29a hsa-miR-21* hsa-miR-29c	IRF2 LHX2 PROX1 SP3 SPIB NFE2 NFE2L2 GATA3 PKNOX1 EBF1 EHF PRDM1 RFX2 RXRB SOX7 FOXO3 FOXP2 TFAP4 THRB TP63 IRF7 USF2 MEF2C MESP1 MLX NFATC1 NFATC4 BCL6 CEBPG
PRKCD	Up-regulated	• intracellular signaling cascade • immune response • lymphocyte mediated immunity • adaptive immune response • adaptive immune response based on somatic recombination of immune receptors built from immunoglobulin superfamily domains	hsa-miR-377 hsa-miR-497 hsa-miR-10b* hsa-miR-195 hsa-miR-221 hsa-miR-26a hsa-miR-181a hsa-miR-217 hsa-miR-136* hsa-miR-657 hsa-miR-29a hsa-miR-222 hsa-miR-20a*	POU2F2 ESR1 NFKB1

			hsa-miR-126 hsa-miR-663 hsa-miR-26b hsa-miR-29c	
PAK1	Up-regulated	• intracellular signaling cascade • protein kinase cascade • MAPKKK cascade	hsa-miR-221 hsa-let-7i hsa-miR-7 hsa-miR-30c	ZFX STAT2 HNF4A NFIX GLI2 YBX1
IQGAP1	Up-regulated	• intracellular signaling cascade • small GTPase mediated signal transduction		ZFX VSX2 STAT2 FOXP2
MAP2K4	Up-regulated	• intracellular signaling cascade • protein kinase cascade • MAPKKK cascade	hsa-miR-141 hsa-miR-200a	HOXA1 NR2C1 ENO1
RASA1	Up-regulated	• intracellular signaling cascade • regulation of cell adhesion • regulation of apoptosis • regulation of cell death	hsa-miR-182 hsa-miR-30c hsa-let-7f-2* hsa-miR-21 hsa-miR-206 hsa-miR-335	IRF3 PRDM1 RXRB HOXA5 SP1

Table 2. The most enriched GO terms accompanied by related *p* values and genes.

IDs	Term	*p* value	Genes	Count
GO:0005794	**Golgi apparatus**	5/62E-05	STX6, CLCN3, SEC24A, B3GALT5, ARFRP1, TRAPPC2L, ARFIP1, ATP6V1B2, BICD2, IL17RD, PNPLA8, COPB2, GLUL, CHST11, RAB11A, SEC22B, CPD, PAK1, RAB10, GOLGA8A, TMCO1, RAB27A, HIP1	23
GO:0019864	**IgG binding**	6/12E-07	FCGR2C, FCGR1B, FCER1G, FCGR2A, FCGR3B	5
GO:0008104	**protein localization**	0/008	STX6, SEC24A, VPS37A, MITD1, ARFIP1, TACC3, MAPK1, COPB2, MIA3, DMD, TRPS1, RAB22A, RAB11A, SEC22B, CD24, RAB10, SEC23IP, RAB27A	18
hsa04666	**Fc gamma R-mediated phagocytosis**	0/006	MAPK1, RAC2, FCGR2C, FCGR2A, PAK1, PRKCD	6

Table 3. The IC_{50} of drugs in single and in combination treatments, and significant statically difference by t-test, CI calculation, and definition.

Cell line	**MTFN IC50** (alone and in combination)	**CURC IC50** (alone and in combination)	***p* Value** (MTFN vs DMSO)	***p* Value** (CURC vs DMSO)	CI	Definition

MCF7	19mM, 11mM	13μM, 5μM	0/0004	0/0005	0/96	additive effect
MDA-MB-231	21mM, 12mM	15μM, 5μM	0/0004	0/0005	0/79	moderate synergism

Figures

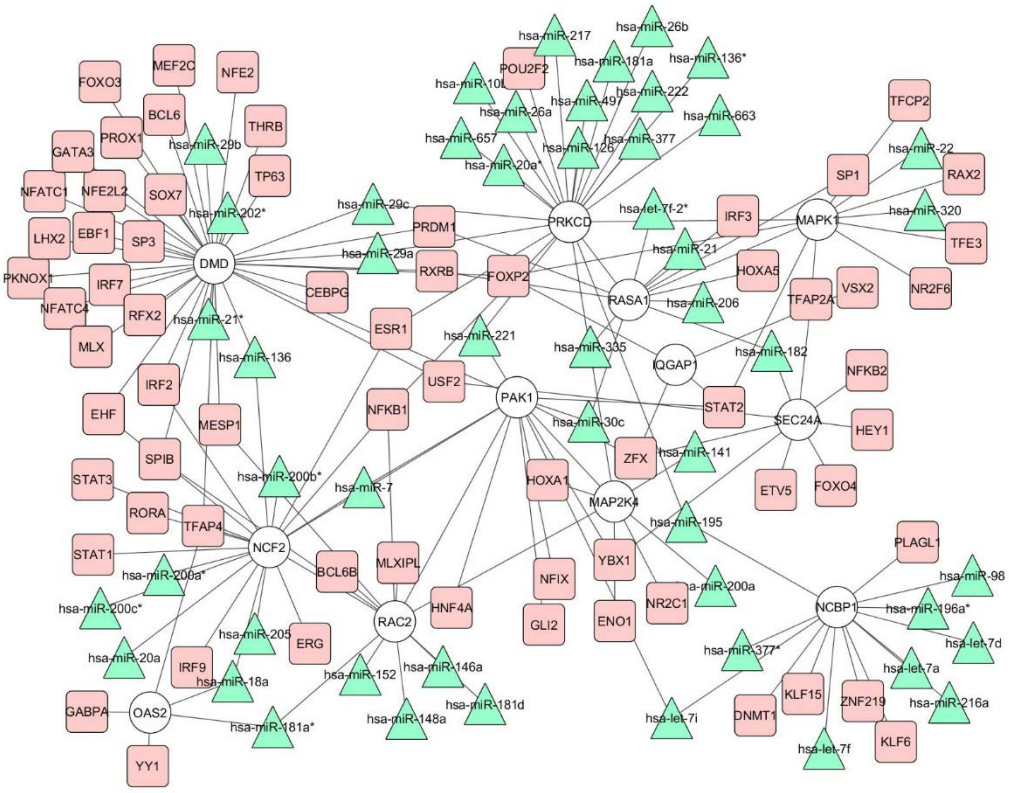

Figure 1. The regulatory network of hubs between BC and DM2. The white, light green, and pink nodes represent co-expressed hubs, miRNAs, and TFs. The network was visualized by Cytoscape 3.6.0. The DMD was the only down-regulated hub while the others were up-regulated.

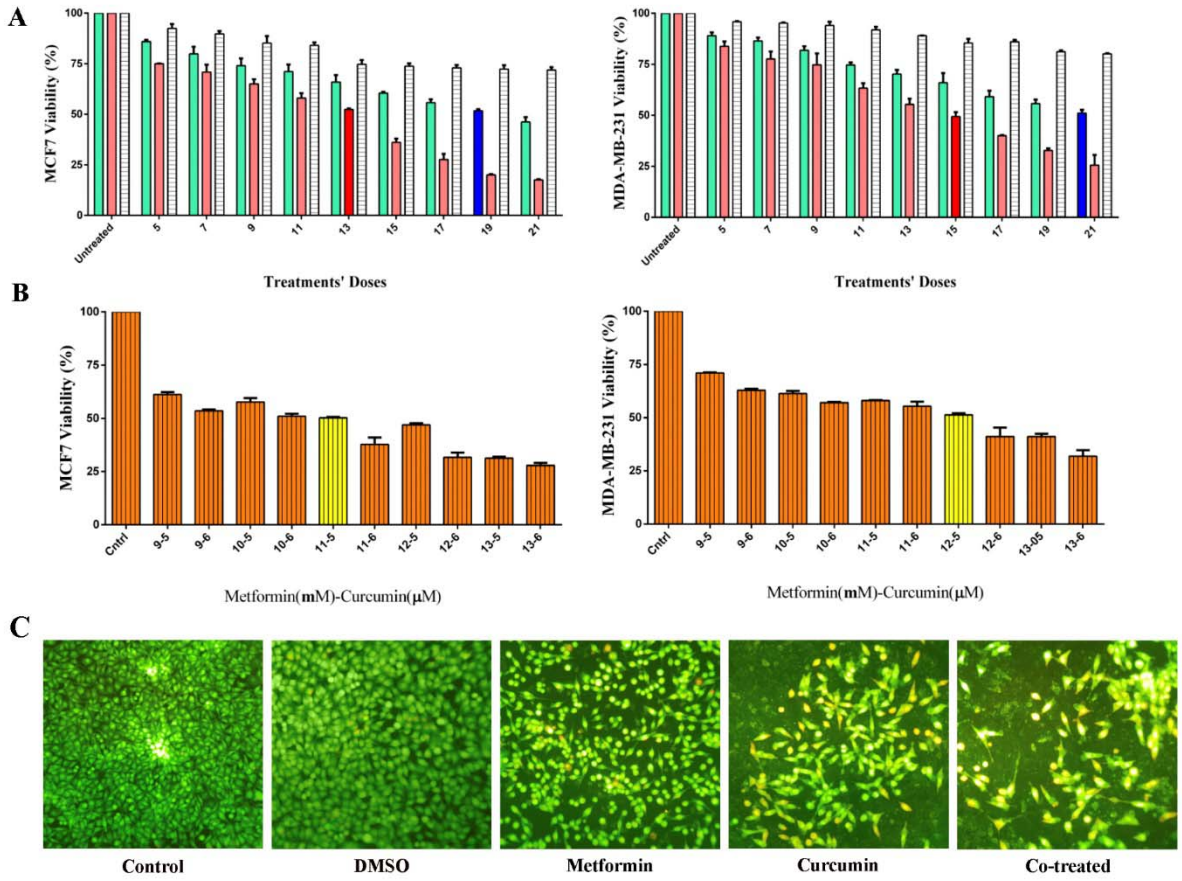

Figure 2. Viability and morphological changes of Treated BC Cells. A and B. Survival plot of treated BC cell lines under MTFN, CURC, DMSO, and MTFN/CURC co-treatment by MTT assay. Each column represents Statistical Reliability (SR) of two independent experiments with their error bars as standard deviation. The cyan columns are MTFN (mM) serial concentrations, pink columns are CURC (μM) serial concentrations, and the white columns represent DMSO. The dark blue and red columns are IC50 of MTFN and CURC respectively. The yellow columns in below plots represent CI50 of co-treatment. The resulted IC50s are highly significant (p value < 0.01) versus DMSO treated and untreated cells as the control groups according to t-test utilization. **B.** Morphological changes of MCF7 under mentioned treatments by AO/EB co-staining. The cells were observed and were magnified 10X and 20X under fluorescent microscope.

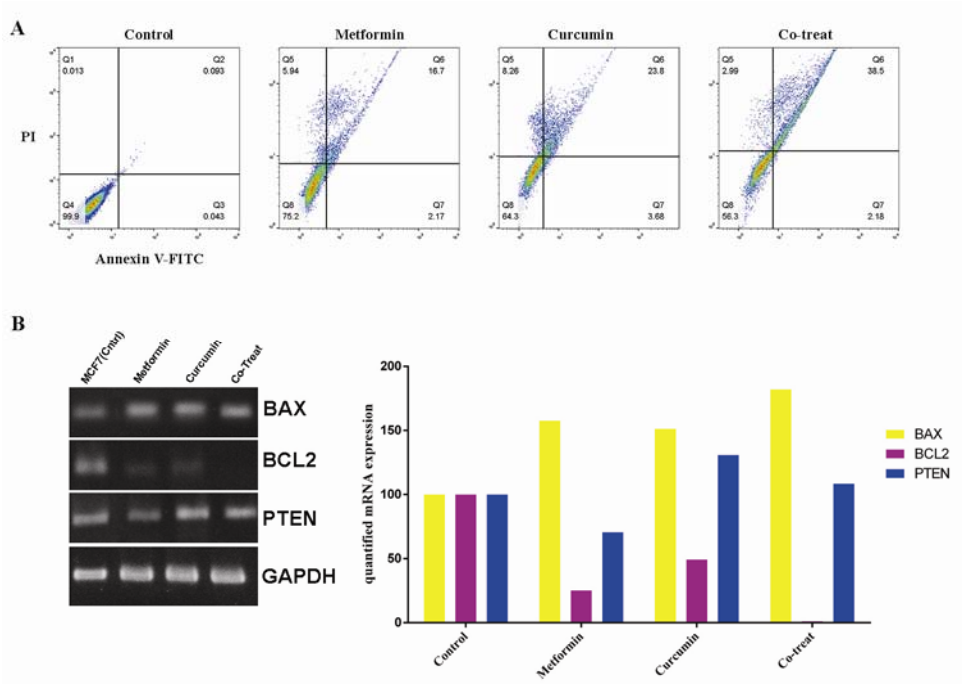

Figure 3. Apoptosis and Gene Expression. A. MCF7 apoptosis by Annexin V-FITC/PI double labeling flow cytometry, treated with IC50 of MTFN, CURC, and their combination after 24h. **B.** Gene expression alteration examined by RT-PCR. The gel electrophoresis image represents expression of candidate gene mRNAs and the graphs were produced by quantification of each band within the image quantified using the ImageJ software and plotted by GraphPad Prism 6. Each column represents SR of quantified mRNA expression.

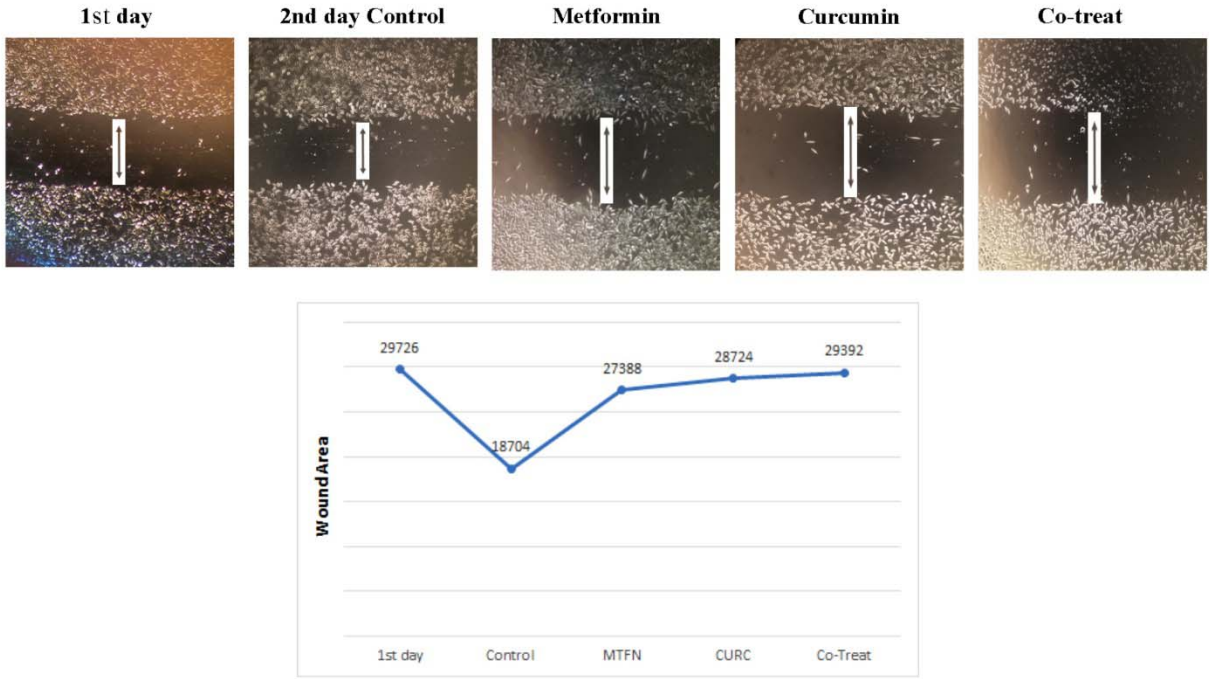

Figure 4. MCF7 migration analysis. MCF7 migration was tested by wound healing assay under IC50 of MTFN, CURC, and their combination treatments after 24h. The cells were observed and were magnified 4X under inverted phase contrast microscope. The quantified wound area was measured and expressed as the space between two sides of cultured cells by ImageJ software.